

# Gene expression profiling on CML patients with Philadelphia translocation

H. ALKHATABI<sup>1,2</sup>, S. ALDAHLAWI<sup>2</sup>, M.S. HAZZAZI<sup>1,2</sup>, R. ALSOLAMI<sup>1,2</sup>, A. ELAIMI<sup>1,3</sup>, M.N. ALMASHJARY<sup>1,2</sup>, R. ALSERIHI<sup>1,2</sup>, H.A. ALKHATABI<sup>4</sup>, M.E. ALOUTHAMI<sup>5</sup>, Y.M. DAOUS<sup>2,6</sup>, S. BAHASHWAN<sup>2,6</sup>, E.B. YASIN<sup>6</sup>, A. BAREFAH<sup>2,7</sup>, F. ALSAYES<sup>2,7</sup>

<sup>1</sup>Department of Medical Laboratory Technology, Faculty of Applied Medical Sciences, King Abdulaziz University, Jeddah, Saudi Arabia

<sup>2</sup>Hematology Research Unit (HRU), King Fahad Medical Research Center, King Abdulaziz University, Jeddah, Saudi Arabia

<sup>3</sup>Center of Excellence in Genomic Medicine Research (CEGMR), King Abdulaziz University, Jeddah, Saudi Arabia

<sup>4</sup>Department of Biochemistry, College of Science, University of Jeddah, Jeddah, Saudi Arabia

<sup>5</sup>GCC Accreditation Center GAC, Jeddah, Saudi Arabia

<sup>6</sup>Department of Medical Laboratory Technology, Faculty of Applied Medical Sciences, King Abdulaziz University, Rabigh, Saudi Arabia

<sup>7</sup>Department of Pathology, Faculty of Medicine, King Abdulaziz University, Jeddah, Saudi Arabia

*H. Alkhatabi and S. Aldahlawi contributed equally as first authors*

**Abstract. – OBJECTIVE:** The use of tyrosine kinase inhibitors (TKIs) and other targeted therapeutics plays a pivotal role in treatment management for individuals diagnosed with chronic myeloid leukemia (CML). However, some patients may experience fewer favorable outcomes and treatment resistance. Our work aims to use whole transcriptome sequencing to evaluate the variations in gene expression patterns among individuals with CML based on their response to TKI therapy.

**PATIENTS AND METHODS:** Ten blood samples were obtained from two groups of patients diagnosed with CML: those at the initial diagnosis stage and those at the recurrence stage. RNA extraction was performed on all samples and used for next-generation sequencing. The data analysis was performed using the DESeq2 R program.

**RESULTS:** In total, 499 genes were identified as having statistically significant differences in expression levels between the two groups. Of these, 122 genes exhibited upregulation, and 377 genes exhibited downregulation. We observed a notable dysregulation in the expression levels of NTRK2 (with a fold change more significant than +5). A significant proportion of the genes that were expressed demonstrated involvement in several biological processes, including the cell cycle, PI3K-AKT signaling system, cellular senescence, oxidative phosphorylation, microRNA in cancer, FOXO signaling pathway, P53 signaling pathway, and other related pathways.

**CONCLUSIONS:** The results demonstrate a correlation between signaling pathways and the development of treatment resistance in pa-

tients with CML. These pathways exhibited enhanced efficacy in transmitting signals downstream of the TKI target, BCR-ABL. Several target genes require additional validation in a more extensive cohort study to verify their correlation with TKI resistance. The present research highlights that many BCR-ABL-independent pathways may be correlated with resistance, thus enhancing the prospective therapy options for patients with CML.

*Key Words:*

Chronic myeloid leukemia (CML), Philadelphia, Tyrosine kinase inhibitor (TKI), Gene expression, Next-generation sequencing.

## Introduction

Chronic myeloid leukemia (CML) has a rich historical background, beginning with the identification of the “Philadelphia chromosome” by Nowell and Hungerford in 1960<sup>1</sup>. This finding significantly advanced the comprehension of chromosomal abnormalities in the context of leukemia. The Philadelphia chromosome was later determined to be the outcome of a balanced reciprocal translocation between chromosomes 9 and 22, denoted as t(9;22)(q34; q11). This translocation leads to the formation of the BCR-ABL1 fusion gene<sup>2</sup>. The BCR-ABL1 fusion protein has heightened tyrosine kinase activity, resulting in

abnormal signal transduction, cell cycle dysregulation, and apoptosis suppression, ultimately promoting the development of leukemia<sup>3-6</sup>.

The discovery of tyrosine kinase inhibitors (TKIs) as a targeted therapy for BCR-ABL fusion has significantly impacted the treatment of patients with CML by transforming the therapeutic approach. The introduction of small-molecule TKIs impacted this further. These TKIs act by impeding the proliferation of the malignant clone by disrupting the connection between the BCR-ABL1 oncogene and adenosine triphosphate (ATP)<sup>7,8</sup>. TKIs are crucial for enhancing the overall survival rate of patients diagnosed with CML. Imatinib, a first-generation TKI, established the fundamental basis for later therapeutic approaches by effectively suppressing the activity of BCR-ABL1 kinase, yielding notable clinical results<sup>9,10</sup>. Second-generation TKIs, including dasatinib, nilotinib, and bosutinib, provided additional treatment options for patients who became resistant or intolerant to imatinib<sup>11</sup>. Third-generation TKIs, like ponatinib and asciminib, have emerged as effective solutions against BCR-ABL1-resistant mutations, offering new treatment avenues<sup>12</sup>.

Despite the efficacy observed with targeted therapy, a specific group of CML patients demonstrate treatment resistance and disease progression that cannot be attributed to BCR-ABL1 gene mutations. This underscores the significance of BCR-ABL1-independent pathways in disease development<sup>13</sup>. Such behavior is influenced by various factors, including the bone marrow microenvironment, genetic and epigenetic changes, alternate signaling pathways, and clonal evolution<sup>14</sup>. Understanding these pathways is important for developing novel treatment options that address BCR-ABL1-independent treatment resistance<sup>15</sup>. Less than 10% of patients demonstrate TKI resistance. The development of disease persistence and treatment resistance can be influenced by several distinct circumstances<sup>16</sup>. TKI resistance has been linked to BCR-ABL mutations, increased expression of drug targets, aberrant drug metabolism, activation of signaling cascades, impaired DNA repair and genomic instability, malfunctions in epigenetic regulation, persistence of leukemia stem cells, and compromised immune system function, among other causes. These resistance mechanisms can be broadly categorized into two groups: those dependent on BCR-ABL and those independent of BCR-ABL.

The analysis of gene expression profiling can elucidate potential associations between the ex-

pression of specific genes and the development of diseases or therapy resistance. It is imperative to ascertain the gene expression profile in patients with CML who are positive for the Philadelphia chromosome. Regarding the various transcript types of BCR-ABL, numerous studies<sup>16-19</sup> indicate that these variants are linked to variations in the clinical and hematological features exhibited by CML patients. Variations in gene expression across several transcripts might lead to divergent tyrosine kinase activity, influencing treatment response. The use of dysregulated pathway identification and gene function cluster analysis can potentially enhance the comprehension of illness pathophysiology<sup>17,18</sup>. Therefore, it is important to use molecular testing and gene expression profiling to advance personalized medicine, wherein treatment strategies are tailored based on individual genetic data<sup>19</sup>.

The genetic profile associated with CML patients in Saudi Arabia remains insufficiently understood. To the best of our current knowledge, there is a dearth of local research regarding gene expression, highlighting the need for further investigation in this area. With this objective in mind, our research investigates gene expression profiles in CML patients who resist TKI therapy. We used a high-sensitivity technology for this investigation, namely RNA sequencing using next-generation sequencing methodologies. Our findings suggest that identifying distinct biomarkers has the potential to elucidate the fundamental factors contributing to treatment resistance. This could enhance the effectiveness of drugs and offer a novel therapeutic approach to enhance treatment outcomes. Additionally, the findings provide valuable insights for researchers regarding developing targeted therapies tailored to individual patients with CML within the studied population.

## Patients and Methods

### *Patient Samples*

Ten peripheral blood samples were collected from CML patients who were positive for Philadelphia at the diagnostic stage (n=5) and after treatment (n=5). Two patients who exhibited complete molecular remission after treatment were considered as controls (remission group), and three patients who relapsed after treatment were considered the relapsed group. The King Abdul-Aziz University Hospital provided the orig-

inal samples, and the hospital's medical records were used to gather clinical data about the patient samples. Results from the Center of Excellence for Genome Medicine Research's molecular lab were used. Patient samples were collected following the ethical approval by KAMC IRB registered at the National BioMedical Ethics Committee, King Abdulaziz City for Science and Technology (Registration No. H-02-K-001). Results from CEGMR molecular lab were used in compliance with Ethics approval obtained (Bio-ethical approval code: 01-CEGMR-Bioeth-2019).

### **RNA Extraction**

RNA was isolated from whole blood using the Qiagen QIAamp RNA Blood Mini Kit (50), Catalog #52304. This method relies on the fundamental principle of RNA extraction, which consists of three stages: cell lysis and protein digestion, washing, and elution. The method was performed in line with the manufacturer's instructions. The extraction was done by transferring the patient's sample into a 15-ml tube and adding an equal volume of 0.9% sodium chloride solution. Mix the solution gently by inverting. Add 5 ml of Histopaque to a new 15 ml conical tube. The tube was centrifuged at 700 g (1,975 rpm) for 30 minutes at room temperature (no brake). Then, the white blood cell (WBC) layer was gently transferred into a new 15 ml tube. Normal saline (0.9% sodium chloride) was added up to 10 ml, and then the tube was centrifuged for 10 minutes at 2,500 rpm at room temperature. Following that, 600 µl of buffer RLT (Buffer RLT is a lysis buffer for lysing cells and tissues prior to RNA isolation and simultaneous RNA/DNA/Protein isolation. When following RNeasy Plus or AllPrep DNA/RNA procedures, Buffer RLT Plus should be used). and 10 µl of β-mercaptoethanol were mixed with the cell pellet. The lysate was homogenized by vortexing for 1 min. For the wash steps, add 600 µl of 70% ethanol, mix, transfer it to the QIAamp RNeasy spin column in a 2 ml collection tube, and centrifuge it for 15 s at 8,000 g (14,000 rpm). In the subsequent stage, the collection tube was employed instead of the flow-through. The RNeasy spin column was then filled with 700 µl of buffer RW1, and the spin column membrane was washed by centrifuging the mixture for one second at 8,000 g (14,000 rpm). The RNeasy spin column was then filled with 500 µl of buffer RPE, and the spin column membrane was washed by centrifuging the mixture for one sec-

ond at 8,000 g (14,000 rpm). The flow-through was thrown out. After washing the spin column membrane for three minutes at 8,000 g (14,000 rpm), 500 µl of buffer RPE was introduced to the RNeasy spin column. Finally, the RNeasy spin column was added onto 1.5 ml tube and RNA was isolated by adding 50 µl of RNase-free water straight to the spin column membrane and centrifuging for 1 minute at 8,000 g (14,000 rpm). The purity of the extracted RNA was evaluated using NanoDrop. The quality was assessed at 260-280 nm absorbance, and a ratio of 1.8 to 2 was considered acceptable.

### **RNA Sequencing**

RNA samples were prepared for RNA sequencing. RNA libraries were sequenced using contemporary Illumina NovaSeq platforms with TruSeq Stranded mRNA panels. Sample quality control (QC) was the first step in the project workflow to ensure that the samples fulfilled the requirements of the RNA-Seq technology. For total RNA samples, preliminary QC was assessed using agarose gel electrophoresis and Nanodrop. Nanodrop was used to determine sample quantitation, and Agilent 2100 (Agilent Technologies, Inc., Santa Clara, CA, USA) was used to assess sample integrity. mRNA Purification and fragmentation were achieved using polyA with oligo-dT beads according to the manufacturer's instructions. Fragmented samples underwent first-strand copy DNA (cDNA), also called complementary DNA, synthesis. Reverse transcriptases (SuperScript II) and random primers converted cleaved RNA fragments primed with random hexamers into first-strand cDNA. Following this, second-strand cDNA synthesis was performed. This process generates double-stranded cDNA by removing the RNA template and generating a replacement strand using dUTP (an enzyme that catalyzes the chemical reaction  $dUTP + H_2O \rightleftharpoons dUMP + \text{diphosphate}$ ) rather than deoxythymidine triphosphate (dTTP). The second strand is quenched by the inclusion of dUTP during amplification, as the polymerase cannot integrate past this nucleotide. AMPure XP (Beckman Coulter, Inc., USA) beads then isolate the ds cDNA from the second-strand reaction mixture. This process results in blunt-ended cDNA.

For end repair, cDNA was mixed with End Repair Mix and AMPure XP beads, followed by ligation with a single "A" nucleotide added to the 3' ends of the blunt segments to prevent

them from ligating to one another. The 3' end of the adapter had a matched single "T" nucleotide that formed a complementary overhang for ligating the adaptor to the fragment. The ends of the double-stranded cDNA were then ligated to several indexing adapters. DNA fragments were enriched using PCR Primer Cocktail to prepare them for hybridization onto a flow cell. All steps were performed according to the manufacturer's instructions, and the library was sequenced on the Illumina NovaSeq 6000 to yield paired-end reads.

### Bioinformatics and Statistical Analysis

After the library was sequenced, clean data were created by removing reads that contained adapters from the base-calling files produced by Illumina sequencers and converting them to FastQ files. Clean reads were aligned using Hisat2 v2.0.5 to the NCBI36/hg18 reference human genome database. Paired-end clean reads were also aligned. Feature Counts v1.5.0-p3 (Bioconductor, Inc., Boston, MA, USA) was used to determine the read counts for each gene. To estimate gene expression levels, the fragments per kilobase of transcript sequence per million base pairs sequenced (FPKM) for each gene were calculated using its length and the number of reads that matched it. Differential expression analysis between the two groups was performed using the DESeq2 R package (v1.20.0) (Free Software Foundation, Inc., Boston, MA, USA). The Benjamini and Hochberg method was used to modify the

calculated  $p$ -values in order to reduce the false discovery rate<sup>6</sup>. Differentially expressed genes were those found by DESeq2 that had an adjusted  $p$ -value lower than 0.05. The cluster Profiler R package implemented a study of the Gene Ontology (GO) enrichment of differentially expressed genes that corrected the gene length bias. The statistical enrichment of differentially expressed genes was examined using KEGG pathways (<http://www.genome.jp/kegg/>). In the DO (Disease Ontology) pathways, a database that explains how human genes function and diseases are classified, genes with a corrected  $p$ -value lower than 0.05 were considered to be significantly enriched by differential expression.

## Results

### CML Patient Cohort

We screened the gene expression of the 10 samples collected from the included Philadelphia-positive CML patients using an Illumina TruSeq stranded mRNA panel (Illumina, Inc., Santa Clara, CA, USA). Two patients were in remission after treatment and were considered controls (remission group: p.1 and p.2), and three patients relapsed after treatment (relapsed group: p.3, p.4, and p.5). Despite the strict quality criteria applied, three samples had to be excluded due to the low-quality concentration of the RNA extraction (p.1-1, p.2-2, and p.3-1). The sample groups are listed in Table I.

**Table I.** Patients' clinical information and list of samples.

#	Sample ID	Treatment	Sample status	Age	Gender	BCR/ABL
1	p1-1	Imatinib	Group 1	26	Female	P210
2	p1-2	Imatinib	Group 2	28	Female	
3	p2-1	Imatinib	Group 1	52	Male	P210
(b3a2)						
4	p2-2	Imatinib	Group 2	58	Male	
5	p3-1	Imatinib	Group 1	43	Female	P210
(b3a2)						
6	p3-2	Imatinib	Group 2	45	Female	
7	p4-1	Imatinib	Group 1	27	Male	P210
(b2a2)						
8	p4-2	Imatinib	Group 2	29	Male	
9	p5-1	Imatinib	Group 1	19	Female	P210
(b2a2)						
10	p5-2	Imatinib	Group 2	22	Female	

\*p1 and p2 are used as control samples (patients who achieve complete molecular remission), p3, p4, and p5 are relapsed patients. Although each patient had two samples before (at diagnosis) and after (treatment), Group 1 are samples at diagnosis, and Group 2 are samples after treatment with TKIs.



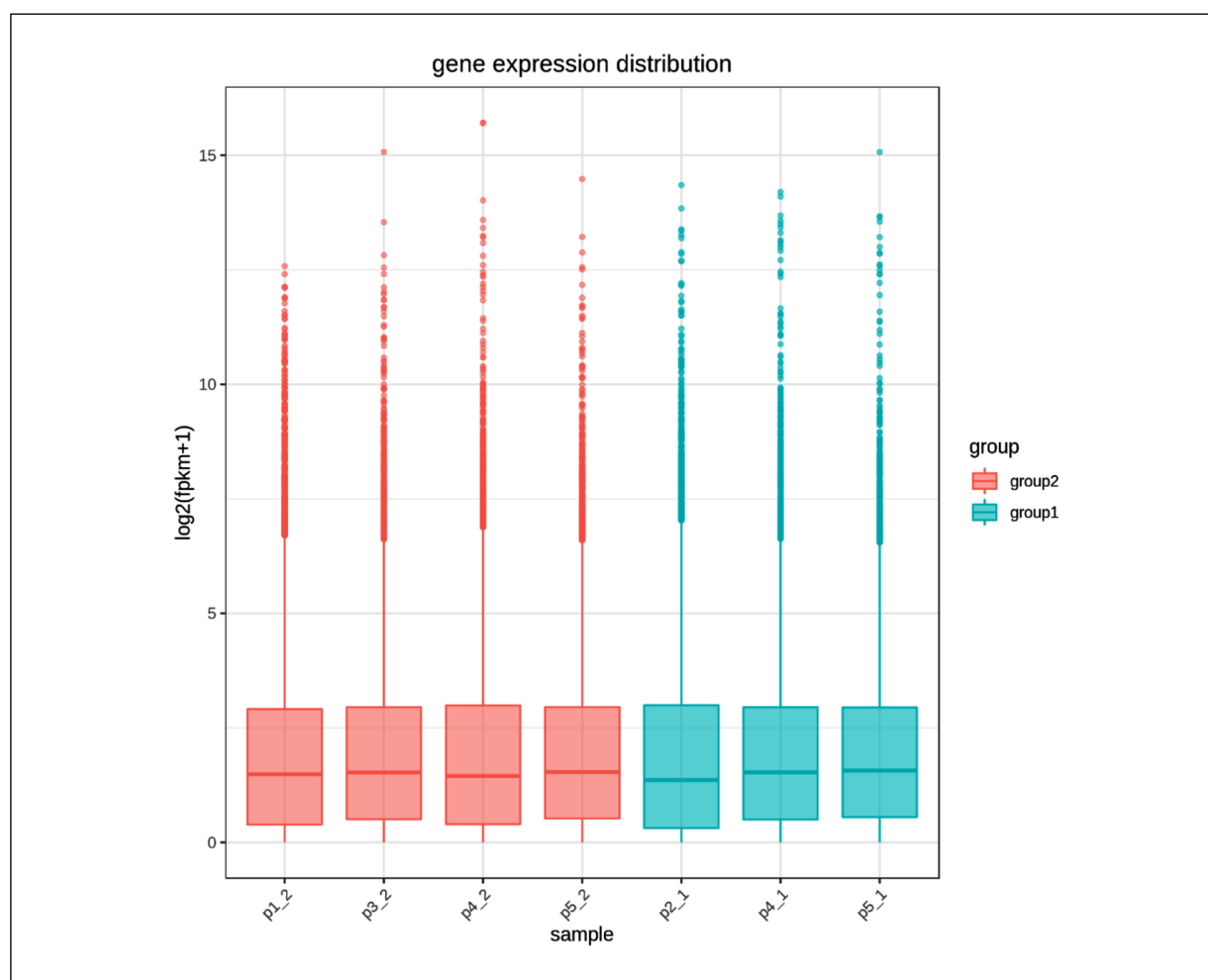


**Figure 1.** Sample gene expression distribution box plot. Group 1: samples at diagnosis, group 2: samples after treatment. X-axis: represents the name of the sample. Y axis: indicates the  $\log_2$  (FPKM+1).

### Gene Expression Distribution

The gene expression level was estimated by FPKM, a method that accounts for the impact of sequencing depth and gene length on fragment count. We were able to determine the amount of gene expression<sup>6</sup>. Boxplots were used to depict the distribution of gene expression levels and FPKM among several samples (Figure 1).

### Cluster Analysis

All the differentially expressed genes in the comparison groups were pooled as the differential gene set. Hierarchical clustering was performed to compare gene expression profiles in all samples and between groups. The heatmap demonstrated distinct gene expression signatures for the gene expression profiles (Figure 2). Strong differences were observed in the respective signatures for group 1 (be-

fore treatment) and group 2 (after treatment). We observed uniquely high gene expression in samples p.1-2, p.3-2, p.4-2, and p.5-2. Differences in expression were observed between the control remission samples (p.2-1: as control at diagnosis and p.1-2: as control at remission) and the resistant samples (p.4-1, p.5-1, p.4-2, p.3-2, and p.5-2). Based on the expression pattern, there were some differences in the overall expression pattern between the control at remission sample and the relapse samples, as well as between the control at diagnosis sample and samples at diagnosis.

### Differential Gene Expression Analysis

Following the quantification of gene expression between the samples of the two groups (before and after treatment), the differential expression of 28,659 genes was identified using the

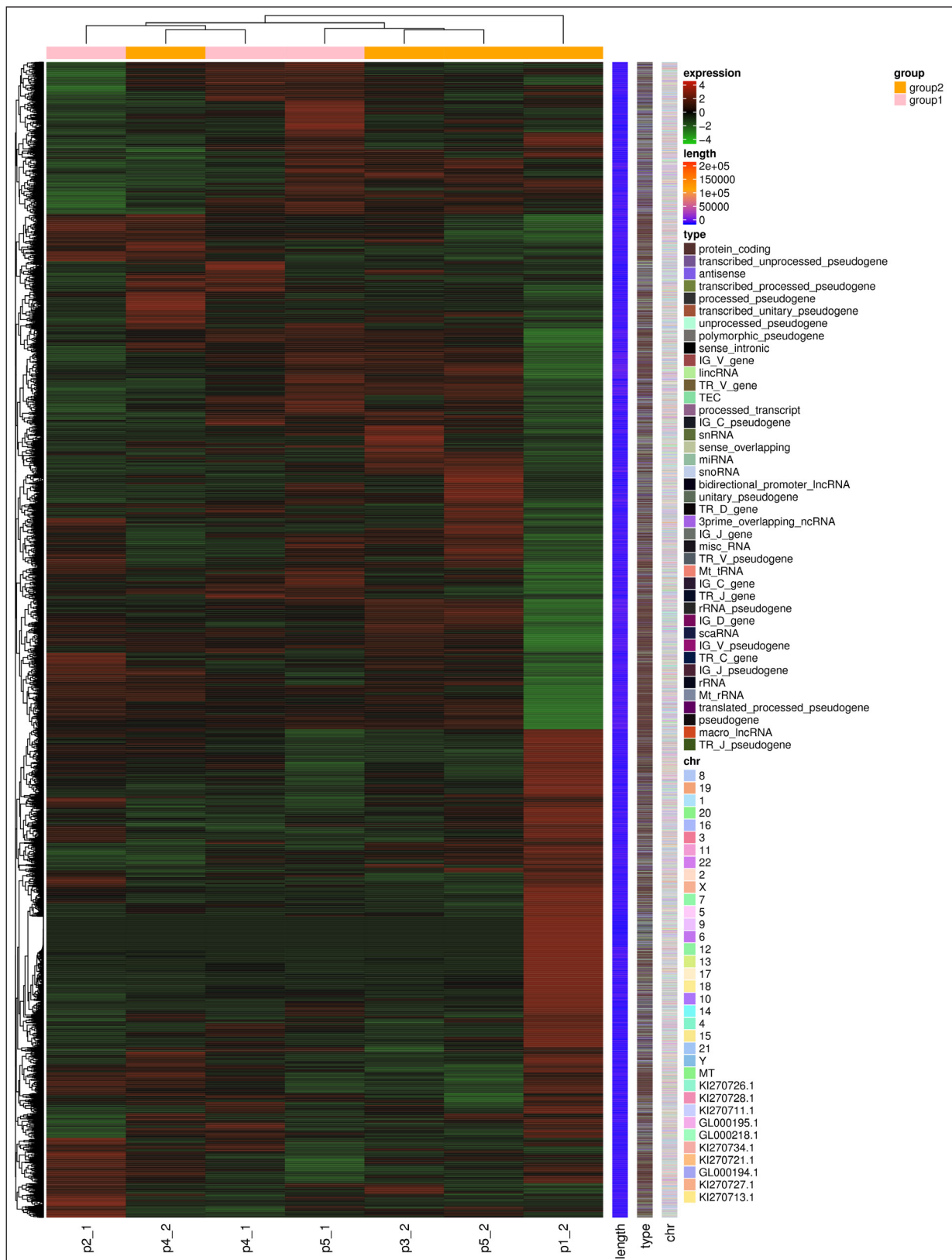


**Figure 2.** Differential gene expression heatmap clustering. Red color indicates genes with high expression levels, and green color indicates genes with low expression levels. The color ranging from red to green indicates that  $\log_2(\text{FPKM}+1)$  values where from large to small, and the biological type of the gene is also added to the heatmap.

**Table II.** Differential gene expression results.

Compare	All	Up	Down	Threshold
Group 1 vs. group 2	499	122	377	DESeq2 $p$ -value $\leq 0.05$ $ \log_2\text{Fold Change}  \geq 1.0$
p3_2 vs. p1_2	11,245	5,993	5,252	edgeR $p$ -value $\leq 0.05$ $ \log_2\text{Fold Change}  \geq 1.0$
p4_1 vs. p2_1	5,503	3,384	2,119	edgeR $p$ -value $\leq 0.05$ $ \log_2\text{Fold Change}  \geq 1.0$
p4_2 vs. p1_2	9,403	4,797	4,606	edgeR $p$ -value $\leq 0.05$ $ \log_2\text{Fold Change}  \geq 1.0$
p5_1 vs. p2_1	6,936	4,123	2,813	edgeR $p$ -value $\leq 0.05$ $ \log_2\text{Fold Change}  \geq 1.0$
p5_2 vs. p1_2	11,221	6,281	4,940	edgeR $p$ -value $\leq 0.05$ $ \log_2\text{Fold Change}  \geq 1.0$

DESeq2 R package version 1.20.0 (Free Software Foundation, Inc.). The overall comparison of  $\log_2\text{FoldChange}$  indicates the ratio of gene expression levels between the before-treatment group (group 1) and the after-treatment group (group 2). The thresholds for screening and statistics for the number of differential genes (including up- and down-regulated genes) for each comparison

group are displayed in Table II. A volcano curve demonstrated that approximately 377 genes were downregulated, and 122 genes were upregulated, with a 2-fold change in expression and a  $p$ -value of 0.05 (Figure 3). Our data revealed that 499 genes had a significant  $p$ -value of 0.05 and demonstrated a 75% downregulation in expression compared to the groups.

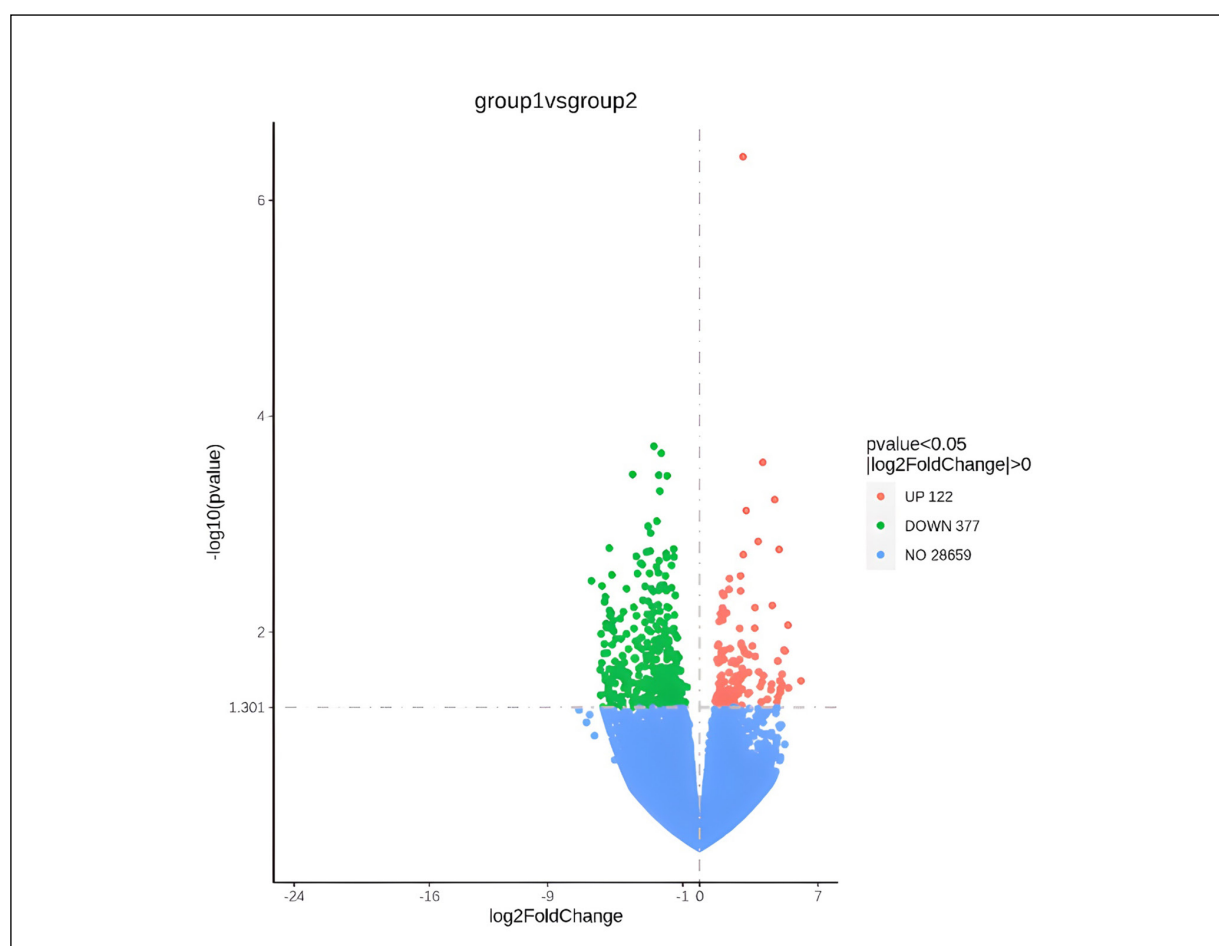


**Figure 3.** Volcano plots show the overall distribution of differentially expressed genes. The blue color represents the total genes differentially expressed (28659). Red dots represent up-regulation genes (122). Green dots represent down-regulation genes (377).

**Table III.** Up-regulated gene expression, more than +3-foldChange was considered up-regulation gens expression at  $p$ -value < 0.05.

#	Gene name	log <sub>2</sub> FoldChange	p-value
1	<i>HTRA1</i>	3.12187	0.013492
2	<i>AC104623.1</i>	3.255878	0.009212
3	<i>FAM156A</i>	3.273884	0.005947
4	<i>AC134349.1</i>	3.282123	0.016823
5	<i>RASD1</i>	3.457243	0.001448
6	<i>FOXD4</i>	3.497352	0.023391
7	<i>RF00019</i>	3.58509	0.031975
8	<i>AC005244.1</i>	3.647371	0.044425
9	<i>ZNF311</i>	3.683641	0.029043
10	<i>AC024361.3</i>	3.766341	0.025314
11	<i>AL356272.1</i>	4.003904	0.042079
12	<i>RN7SL749P</i>	4.212191	0.034307
13	<i>HAPI</i>	4.260843	0.030464
14	<i>CCL2</i>	4.293784	0.005667
15	<i>SHD</i>	4.438903	0.000594
16	<i>KCNK10</i>	4.57531	0.044507
17	<i>AC105046.1</i>	4.619638	0.018581
18	<i>AL670729.3</i>	4.639695	0.039946
19	<i>DCLK2</i>	4.698051	0.001719
20	<i>APOF</i>	4.744285	0.028294
21	<i>AL390026.1</i>	4.76109	0.036451
22	<i>AC005740.3</i>	4.778081	0.033497
23	<i>AC007938.2</i>	4.877477	0.024653
24	<i>AC092896.2</i>	4.888765	0.030994
25	<i>NTRK2</i>	5.049878	0.015012
26	<i>AC112184.1</i>	5.223346	0.008637
27	<i>CSTPI</i>	5.260079	0.03308
28	<i>RFPL4A</i>	5.995737	0.028335

**Table IV.** Down-regulated gene expression, less than -3-foldChange was considered down-regulation gene expression (+3 > 0 > -3), at  $p$ -value < 0.05.

#	Gene name	log <sub>2</sub> FoldChange	p-value	#	Gene name	log <sub>2</sub> FoldChange	p-value
1	<i>MROH7</i>	-6.41064176	0.003358135	76	<i>CYP3A4</i>	-4.30423114	0.023951532
2	<i>BGLT3</i>	-5.891827882	0.02234981	77	<i>AL121672.3</i>	-4.29635903	0.023735191
3	<i>HBBP1</i>	-5.862393396	0.03847081	78	<i>AC098824.1</i>	-4.26569869	0.029180112
4	<i>HIST1H2AH</i>	-5.834693662	0.010431846	79	<i>SAGE1</i>	-4.24886831	0.033501623
5	<i>ENTPD8</i>	-5.799111934	0.01932821	80	<i>AC131097.4</i>	-4.2486163	0.037584255
6	<i>KRT17</i>	-5.778513442	0.003739775	81	<i>RNA5-8SN2</i>	-4.23538579	0.031883883
7	<i>LINC01585</i>	-5.726518264	0.049726661	82	<i>KCNH4</i>	-4.23401112	0.027659479
8	<i>AP006545.2</i>	-5.664028848	0.015879618	83	<i>AL138976.2</i>	-4.21804856	0.01435956
9	<i>LINC01819</i>	-5.640236884	0.01292101	84	<i>SLC34A2</i>	-4.21434292	0.024176077
10	<i>AC006449.2</i>	-5.631348175	0.00524883	85	<i>TAS2R10</i>	-3.9878903	0.044665932
11	<i>HOXB-AS2</i>	-5.596372104	0.025240512	86	<i>ARHGAP23</i>	-3.96946062	0.000346234
12	<i>SV2B</i>	-5.591560113	0.02777446	87	<i>AC004975.2</i>	-3.95196213	0.02958614
13	<i>CTHRC1</i>	-5.581904963	0.00473056	88	<i>AC104389.5</i>	-3.91858549	0.049200036
14	<i>EIFIP4</i>	-5.550119204	0.027947211	89	<i>PTH2R</i>	-3.90347084	0.005912355
15	<i>CRYZP1</i>	-5.534037188	0.00838237	90	<i>AC012065.5</i>	-3.88737416	0.039970672
16	<i>MAMDC2-AS1</i>	-5.526007318	0.009095099	91	<i>SLC2A1-AS1</i>	-3.8868618	0.009272318
17	<i>CRYM-AS1</i>	-5.499877578	0.037333104	92	<i>RAB42</i>	-3.87209152	0.048331829
18	<i>AC087481.1</i>	-5.466355214	0.015584113	93	<i>AC091563.1</i>	-3.86264323	0.01750896
19	<i>CLDN3</i>	-5.416844424	0.034239146	94	<i>AP001830.1</i>	-3.83445128	0.041689035

Continued



**Table IV (Continued).** Down-regulated gene expression, less than -3-fold change was considered down-regulation gene expression (+3 > 0 > -3), at  $p$ -value < 0.05.

#	Gene name	log <sub>2</sub> FoldChange	p-value	#	Gene name	log <sub>2</sub> FoldChange	p-value
20	<i>LINC01952</i>	-5.387311096	0.031572416	95	<i>AC022509.2</i>	-3.82601228	0.017822119
21	<i>AP001099.1</i>	-5.353390521	0.022095987	96	<i>TRPM5</i>	-3.82485	0.017339277
22	<i>RBI-DT</i>	-5.350845131	0.001671749	97	<i>GGNBP1</i>	-3.81832796	0.041543107
23	<i>RN7SL5P</i>	-5.338658535	0.041943214	98	<i>AC017083.1</i>	-3.79300239	0.045723565
24	<i>AL157371.2</i>	-5.338285859	0.037224267	99	<i>AC020951.1</i>	-3.79099015	0.01219604
25	<i>PTX4</i>	-5.326498619	0.006335606	100	<i>NR1I2</i>	-3.75810717	0.001990954
26	<i>AC009951.1</i>	-5.32236489	0.009082146	101	<i>PTPN14</i>	-3.74148705	0.007071801
27	<i>NPMIP26</i>	-5.30317559	0.007062707	102	<i>TDRD12</i>	-3.73703049	0.035413828
28	<i>TSLP</i>	-5.298844629	0.048637657	103	<i>AC007613.1</i>	-3.70481707	0.046888233
29	<i>GHET1</i>	-5.239289546	0.006676958	104	<i>AGPAT4-IT1</i>	-3.6825264	0.002878208
30	<i>HIST1H4B</i>	-5.239143116	0.041310163	105	<i>AC025031.4</i>	-3.67891073	0.012050694
31	<i>KRT17P6</i>	-5.2192846	0.046412723	106	<i>SLC2A4</i>	-3.65716558	0.013444269
32	<i>HOXA11-AS</i>	-5.215068156	0.02706281	107	<i>AC006453.2</i>	-3.60354245	0.025267778
33	<i>AL139353.1</i>	-5.207457243	0.008792397	108	<i>PRMT5-ASI</i>	-3.60261275	0.030131672
34	<i>CHRNA3</i>	-5.194101614	0.002960255	109	<i>NPAS1</i>	-3.59793541	0.021813818
35	<i>RBBP4P2</i>	-5.184984321	0.013116922	110	<i>TPTE2</i>	-3.57148945	0.031940992
36	<i>AC021683.2</i>	-5.135315398	0.048787881	111	<i>AL138831.1</i>	-3.56579625	0.04363389
37	<i>AP002364.1</i>	-5.120497979	0.007806394	112	<i>AL009031.1</i>	-3.52970478	0.042643125
38	<i>AC015908.3</i>	-5.114697888	0.025840392	113	<i>BMX</i>	-3.48675056	0.002308226
39	<i>TRGV1</i>	-5.111754906	0.022473418	114	<i>TM4SF1</i>	-3.44409812	0.01122587
40	<i>DUXAP9</i>	-5.110290254	0.023092507	115	<i>CES3</i>	-3.43386008	0.020744969
41	<i>KCNMA1</i>	-5.097549797	0.009829853	116	<i>KIF7</i>	-3.42627282	0.014328934
42	<i>AL135910.1</i>	-5.080901442	0.037323391	117	<i>AL008718.3</i>	-3.39402256	0.048086898
43	<i>TDRD1</i>	-5.073028758	0.047893921	118	<i>BIK</i>	-3.39199143	0.002370937
44	<i>EGOT</i>	-5.072250944	0.023501608	119	<i>MYRIP</i>	-3.38363366	0.031516234
45	<i>NNMT</i>	-5.04101452	0.02254532	120	<i>RPSAP54</i>	-3.38215494	0.029277328
46	<i>AP001767.4</i>	-5.00665933	0.018741626	121	<i>CCDC150</i>	-3.36435471	0.005067853
47	<i>TLCD1</i>	-5.000486092	0.029919927	122	<i>IQCA1</i>	-3.3173332	0.040946819
48	<i>AC244502.3</i>	-4.969028746	0.0115252	123	<i>HOXA-AS2</i>	-3.29618596	0.032692489
49	<i>AL356801.1</i>	-4.885886864	0.025189692	124	<i>DDX11-AS1</i>	-3.2920856	0.041366578
50	<i>AL161910.1</i>	-4.857847799	0.041234737	125	<i>KIAA1257</i>	-3.24373987	0.020893311
51	<i>AF196972.1</i>	-4.78746815	0.020052734	126	<i>ANTXR1</i>	-3.24056315	0.008128877
52	<i>ANO7</i>	-4.783481841	0.02542518	127	<i>ITGA9</i>	-3.23079482	0.003785877
53	<i>COX7A1</i>	-4.737523531	0.022336528	127	<i>AC006042.1</i>	-3.1720525	0.032243741
54	<i>CDC42-IT1</i>	-4.70614276	0.00750818	128	<i>KIF26A</i>	-3.16784532	0.016423993
55	<i>ENPP7P11</i>	-4.6774852	0.043248411	129	<i>MSRB3</i>	-3.15210134	0.00182391
56	<i>RIMBP3C</i>	-4.657652719	0.011528963	130	<i>AC015802.3</i>	-3.14897501	0.027170176
57	<i>AC141424.1</i>	-4.655612711	0.039639148	131	<i>STAR</i>	-3.12128546	0.046162951
58	<i>AC025031.5</i>	-4.65316357	0.047851019	132	<i>AC239803.3</i>	-3.12027089	0.018285356
59	<i>AC015818.6</i>	-4.614521824	0.047397516	133	<i>HEPACAM2</i>	-3.11195525	0.044011899
60	<i>AC022272.1</i>	-4.592176104	0.046098944	134	<i>IL17D</i>	-3.11065625	0.028719271
61	<i>AC010422.1</i>	-4.576700801	0.022362446	135	<i>AL354718.1</i>	-3.09696926	0.012599044
62	<i>A4GALT</i>	-4.572079384	0.043765362	136	<i>SMIM6</i>	-3.09364499	0.04308042
63	<i>CASPI6P</i>	-4.564121906	0.016605051	137	<i>TRIM71</i>	-3.09341138	0.006856433
64	<i>OR14LIP</i>	-4.545520858	0.04993241	138	<i>TBX1</i>	-3.09216849	0.033621984
65	<i>AC127024.8</i>	-4.539946464	0.049121888	139	<i>ATP5PDP4</i>	-3.08497609	0.046694981
66	<i>CYP7B1</i>	-4.516954234	0.006493964	140	<i>NOV</i>	-3.07787509	0.013785167
67	<i>HIST1H1PS1</i>	-4.4967683	0.026671545	141	<i>AC097634.1</i>	-3.06938923	0.039687509
68	<i>AC004832.5</i>	-4.464593002	0.033109579	142	<i>LINC02593</i>	-3.05806804	0.038883127
69	<i>AL121983.2</i>	-4.45721558	0.019180787	143	<i>WDR31</i>	-3.05794187	0.047361039
70	<i>RF00017</i>	-4.443410167	0.027912922	144	<i>AC092821.1</i>	-3.0564152	0.009494064
71	<i>C9orf84</i>	-4.430917687	0.025823942	145	<i>AC004477.1</i>	-3.05452463	0.005184248
72	<i>LINC01268</i>	-4.423954944	0.032743116	146	<i>MATN2</i>	-3.05233231	0.001048299
73	<i>ITFGI-ASI</i>	-4.414705912	0.031655952	147	<i>TRIM6</i>	-3.04819252	0.017348279
74	<i>RNU4-89P</i>	-4.326334469	0.010395261	148	<i>SLC22A20P</i>	-3.01293348	0.006910815
75	<i>AC006511.3</i>	-4.326249877	0.003971808				

The candidate gene set was reduced by selecting the most differentially expressed genes. The cutoff level was adjusted to consider an over +3-fold change in expression as upregulated and less than -3-fold as down-regulated at  $p$ -value  $<0.05$ . This

resulted in a 178-gene set, as shown in Table III and Table IV. Of these 178 genes, 150 demonstrated decreased expression, and 28 demonstrated increased expression in the relapsed patient group compared to the remission patient group. The most

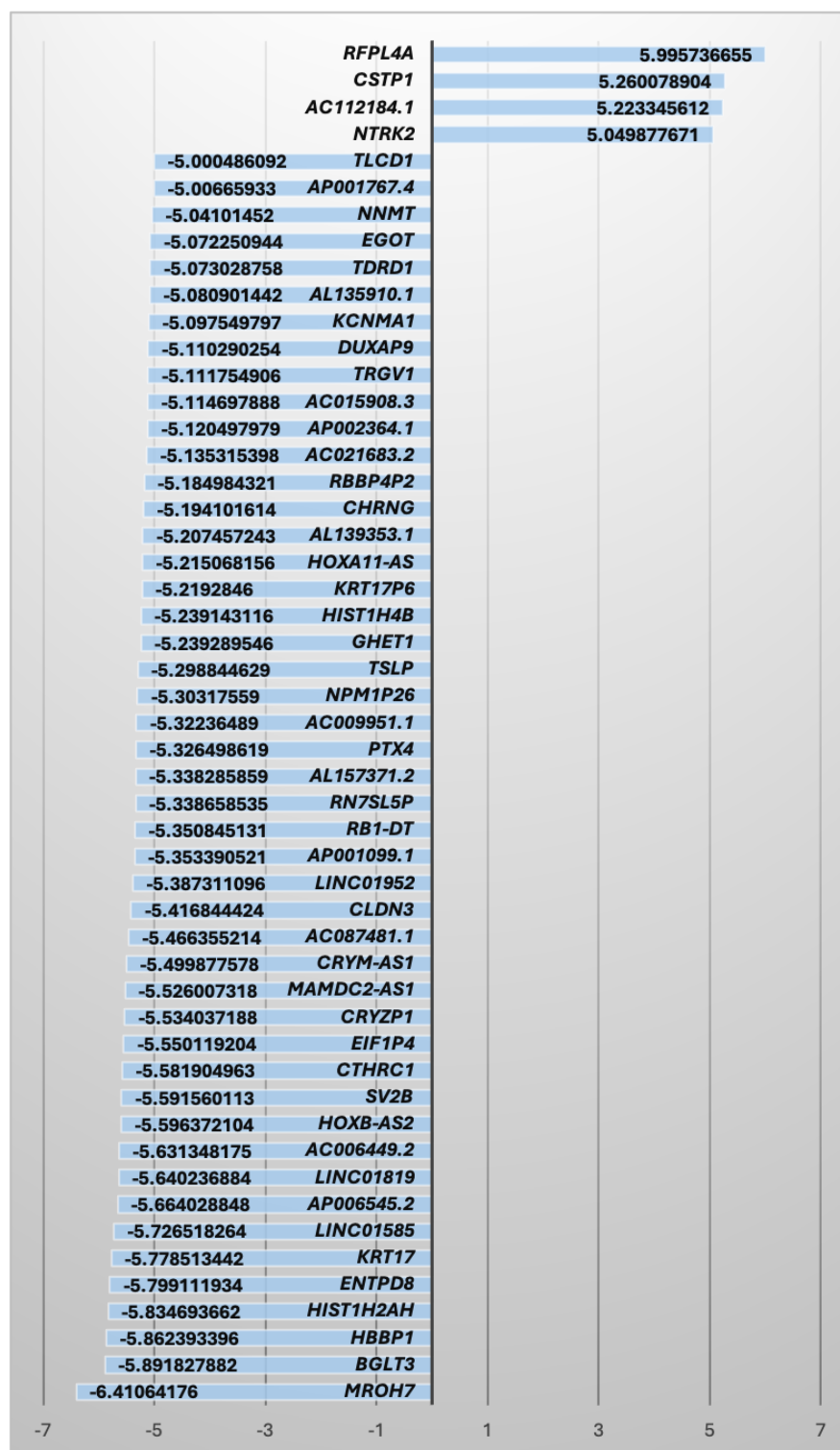


**Figure 4.** The most highly expressed genes were (*RFPL4A*, *CSTP1*, *AC112184.1*, and *NTRK2*) with more than 5-fold change expression. Moreover, many genes were low expressed with less than -5 foldChange, including (*MROH*, *BGLT3*, *HBBP1*, *HIST1H2AH*, *ENTPD8*, and *KRT17*). All at  $p$ -value  $<0.05$ .

highly expressed genes were *RFPL4A*, *CSTPI*, *AC112184.1*, and *NTRK2*, with more than a 5-fold change in expression. Moreover, many genes were associated with a less than -5-fold change, including *MROH*, *BGLT3*, *HBBP1*, *HIST1H2AH*, *ENTPD8*, and *KRT17* (Figure 4).

**Functional Analysis**

We used the clusterProfiler software version 3.8.1 (Qiagen, Germantown, MD, USA) for KEGG enrichment analysis for the enrichment analysis

of the differential expressed genes. The pathway enrichment analysis identified significantly enriched metabolic pathways associated with the differentially expressed genes. Most of the genes were related to cellular metabolic process, and the genes were subsequently determined to be significantly involved in the cell cycle, PI3-AKT signaling pathway, cellular senescence, oxidative phosphorylation, microRNA in cancer, FOXO signaling pathway, and P53 signaling pathway. These results are represented in Figure 5.

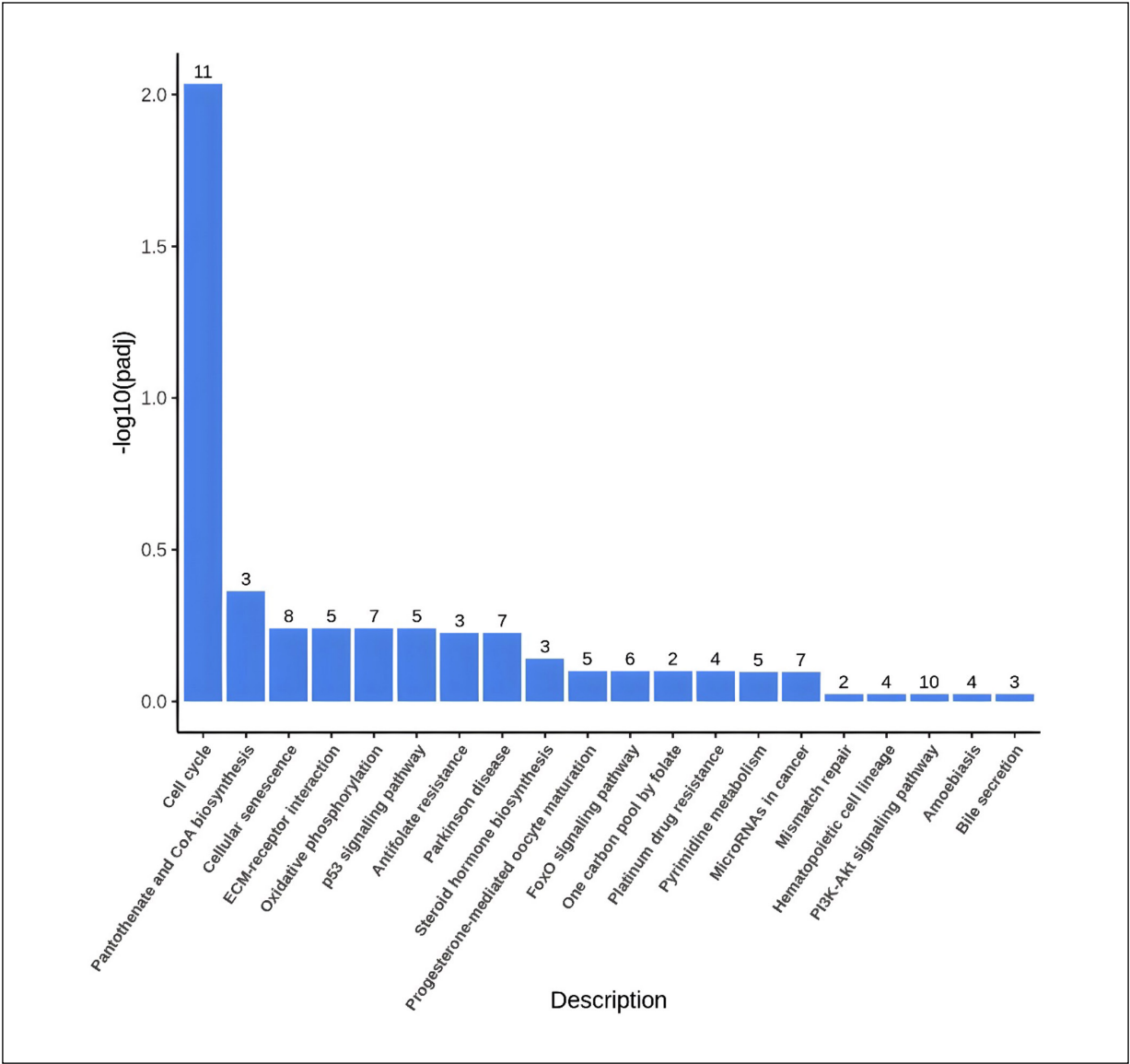


**Figure 5.** The most significant 20 KEGG pathways were selected for display in the KEGG enrichment results. If the results are less than 20, all pathways will be drawn, as shown in the following figure. In this figure, the abscissa is the KEGG pathway, and the ordinate is the significance level of the pathway enrichment. Higher values correspond to higher significance.

## Discussion

TKI-targeted therapies play an essential role in CML patient treatment management. However, some patients experience less favorable outcomes, and treatment resistance might develop *de-novo* or during therapy. Many factors can affect treatment response, including different BCR-ABL transcript types, alterations to the target molecular drug, and alterations in the signaling pathways of leukemic stem cells<sup>10,20,21</sup>. The expression of specific biomarkers characterizes CML leukemic stem cells and may identify specific disease phases. Increased gene activity expression is involved in self-renewal and drug resistance.

Gene expression profiling can highlight the association between gene expressions and disease pathogenesis or treatment resistance. Our study aimed to use whole transcriptome sequencing to assess differential gene expression profiles among CML patients based on responses to TKI-based therapy, as there is currently a lack of knowledge about the genetic expression profiling associated with CML patients in Saudi Arabia.

RNA sequencing was performed on 10 human blood samples collected from CML patients. Three were from CML patients before treatment, three were from patients after treatment, two were from CML control patients who achieved complete molecular remission at the diagnosis stage, and two were from CML control patients who achieved remission after treatment. RNA extraction was performed for all samples, and  $\leq 20$   $\mu$ g of RNA was used for sequencing. The data analysis and differential expression analysis of two conditions/groups were performed using the DESeq2 R package 1.20.0 (Free Software Foundation, Inc.).

The differential expression of a significant number of genes was identified between the two before and after treatment groups. Genes with an adjusted  $p$ -value  $\leq 0.05$  that had a  $|\log_2 \text{FoldChange}| > 0$  in expression were considered differentially expressed. Our data identified 499 differentially expressed genes, with 75% exhibiting downregulation between the groups. The heatmap showed distinct gene expression signatures, as strong differences were observed in the respective signatures for groups 1 (before treatment) and 2 (after treatment). The candidate gene set was reduced by selecting the most differentially expressed genes. Only a few genes were significantly upregulated or downregulated when compared to other genes. In total, 150 genes with decreased expression and 28 genes with increased expression were identified in

the relapsed patient group compared with the remission patient group (control group). The most highly expressed genes with a +5-fold change in expression were *RFPL4A*, *CSTPI*, *AC112184.1*, and *NTRK2*. Other genes exhibited a less than  $-5$ -fold change in expression, including *MROH*, *BGLT3*, *HBBPI*, *HIST1H2AH*, *ENTPD8*, and *KRT17*. Several genes can be associated with treatment resistance, such as *NTRK2*.

*NTRK* is a gene fusion involving a neurotrophic receptor tyrosine kinase. This has been proven to be a therapeutically relevant genomic event that predicts an individual's response to tropomyosin-related kinases (*TRK*) inhibitors. Tyrosine kinases (*TRKA*, *TRKB*, and *TRKC*) encoded by the *NTRK* genes (*NTRK1*, *NRK2*, and *NTRK3*, respectively) play critical roles in central nervous system development, maintenance, and function<sup>22</sup>. *NTRK2* is located on chromosome 9 [cytogenetic location: 9q21.33, genomic coordinates (GRCh38): 84,668,375-85,095,751]. Human tumors with *NTRK* gene fusions have been found at variable frequencies, and point mutations have been identified as a mechanism of acquired resistance to *TRK* inhibition in individuals with *NTRK* gene mutations<sup>23</sup>. Without ligands, this fusion product can activate the *TRK* kinase and its downstream signaling pathways, which may promote cancer development<sup>24</sup>. Over 12 unique mutations in *NTRK2* and *NTRK3* have been reported in primary leukemia samples<sup>25,26</sup>. A mutation with an in-frame deletion of *NTRK1* (*TrkA*) has been reported in a patient with acute myeloid leukemia; a mutation in this gene may directly disrupt kinase function by interfering with ATP-binding sites<sup>27</sup>. Across a panel of over 7,000 patients with hematologic malignancies, a novel *NTRK2* mutation with ETV6 fusion was reported in secondary-AML patients with a history of CLL who demonstrated sensitivity to larotrectinib. The researchers examined the cause of the relapses and discovered that *NTRK2*-ETV6 expression was present in all the various AML subpopulations. The *TRK* fusion negative-AML clone at baseline expanded due to the relapse. Although *TRK* inhibition proved successful in suppressing the *TRK* fusion clone, the sub-clonal nature of the fusion eventually reduced the effectiveness of *TRK* inhibition<sup>28</sup>. However, *NTRK2* gene fusions were found to be the most common in primary CNS malignancies. Other studies<sup>28-30</sup> have shown that *NTRK2* is associated with BCR fusion in glioma, while AML is associated with the fusion gene *ETV6*.

An increased number of studies<sup>31</sup> were conducted on drugs that can inhibit the Trk of the



TKI domain following the discovery of more gene fusions involving the *NTRK* gene. Only a few Trk receptor tyrosine kinase inhibitors have been evaluated in human clinical trials<sup>22</sup>. The TK inhibitor entrectinib is a targeted inhibitor that blocks the activity of *TrkA*, *TrkB*, and *TrkC*. As with other targeted therapies, *Trk* inhibitors may not be successful if secondary resistance develops. As they have only been recently added to the field of cancer treatments, not much is known about the mechanisms that cause resistance<sup>32</sup>. Regardless of patient age or fusion type, *TRK* tyrosine kinase inhibitors produce notable and durable responses in patients with *TRK* fusion cancer, highlighting the importance of clinical routine tests to identify cancers with *NTRK* gene fusions<sup>33</sup>. It is crucial to investigate the relationship between *TRK* inhibitor responses and *TRK* fusion expression further to establish the durability of responses in hematologic malignancies.

Most of the expressed genes identified in the current study are involved in the cell cycle, PI3K-AKT signaling pathway, cellular senescence, oxidative phosphorylation, microRNA in cancer, and the FOXO and *P53* signaling pathways. In total, 499 differentially expressed genes were found using bioinformatic analyses of GEP data. Several significantly enriched pathways were identified between the diagnosis and post-TKI treatment groups. The functional enrichment study revealed that 11 of the 127 genes encoded proteins involved in the cell cycle pathway (*MCM2*, *BUB1*, *CCNB2*, *CCNA2*, *CCNB1*, *CDC6*, *CDK6*, *TTK*, *CDK1*, *ORC1*, and *TFDP2*). Specifically, the genes are involved in the G1, S, and M phases of the cell cycle and in chromosome replication, cell proliferation, DNA replication, and the DNA damage checkpoint. According to previous studies<sup>34</sup>, CML leukemic stem cells exhibit increased expression of multiple genes that encode proteins involved in the cell cycle and chromosome segregation.

The deregulation of genes involved in the PI3K-AKT signaling pathway was also detected. The overexpression of the *EREG*, *IL6*, *ITGA9*, *NTRK2*, *MYB*, *LAMC3*, *CDK6*, *NR4A1*, *BRCA1*, and *LAMB2* genes could indicate the up and down-regulation of cell cycle proliferation and differentiation via the MAPK and mTOR signaling pathways, which are activated by BCR-ABL in CML cells<sup>35</sup>. The mTOR pathway is a component of the PI3K/AKT/mTOR pathway. Imatinib and mTORC1 inhibition work together to cause apoptosis in CML cells<sup>36</sup>. When growth factors and cytokines bind to their specific receptors and

activate these pathways, important downstream molecules are directly activated by BCR-ABL<sup>37</sup>. This stimulates the PI3K pathway, leading to the expression of BCR-ABL in CML progenitors and, therefore, the activation of the mTOR and Akt pathways. BCR-ABL inhibition works in conjunction with mTOR and PI3K inhibition, increasing sensitization to nilotinib and enhancing apoptosis<sup>38</sup>. Similarly, Ras/MAPK signaling activation has been linked to BCR-ABL1-dependent cellular transformation. PI3K/AKT signaling activation has been demonstrated to play a significant role in CML, mediating both the stimulation of cell survival and possibly anti-apoptotic signaling<sup>39</sup>. Overexpression of the Raf/MEK/ERK and PI3K/Akt pathways has been related to worse prognoses in AML. Therefore, developing inhibitors to target these pathways may successfully treat leukemia<sup>37</sup>.

The microRNA (miR-21) level has been shown to be upregulated in CML patient samples when the TKI response was not optimal<sup>40</sup>. In line with this, we identified seven genes that are downregulated in microRNA that are related to cancer (*TRIM71*, *STMN1*, *SOX4*, *CDK6*, *SPRY2*, *BRCA1*, and *PLAU*). Additional research has revealed that imatinib and PI3K inhibition and miR-21 silencing decrease AKT phosphorylation and MYC expression, suggesting that miR-21 mediates its action by controlling the PI3K/AKT axis<sup>41</sup>. In the context of CML, distinct molecular pathways for the downregulation of miRNAs (miR-150 and the miR-29a/b cluster) are well-defined. According to a previous study<sup>42,43</sup> that used samples from patients at various CML stages, lower miR-150 and miRNA-29a/b expression levels were associated with poor prognoses for patients undergoing TKI treatment, suggesting miRNA could be used as a potential biomarker of treatment response.

## Conclusions

TKI treatment has revolutionized CML care and substantially improved patient outcomes; however, drug resistance remains a significant issue. Patients who do not respond well to treatment must be monitored constantly so that new approaches can be tried as quickly as possible. Gene expression analysis may serve as a vital tool for individual patient stratification, as it may be used to discover genetic markers that can be targeted during treatment to improve clinical re-



sults. Here, the next-generation sequencing method identified genes with significant deregulation in relapse patients. The genes merit additional validation to determine whether their monitoring or targeting could improve CML clinical treatment. Most of the genes identified played roles in many physiological processes, such as the cell cycle, the PI3K-AKT signaling system, cellular senescence, oxidative phosphorylation, microRNA in cancer, and the FOXO and P53 signaling pathways. These routes exhibited superior efficacy in transmitting signals downstream of the TKI target, BCR-ABL. This study highlights the possible functions of the candidate genes in CML; however, their precise functions need to be investigated in larger cohort studies. Similarly, the importance of the deregulated genes identified here should be validated to determine their significance in CML. To the best of our knowledge, no other study in Saudi Arabia has used RNA sequencing and gene expression analysis to determine a set of gene signatures and their biological pathways to predict TKI therapy response in CML patients. Our findings provide a potential foundation for developing therapeutic regulation biomarkers based on gene expression profiles.

### Conflict of Interest

The authors declare no conflicts of interest.

### Acknowledgements

This research work was funded by the Institutional Fund Projects (grant no IFPRC-034-140-2020). The authors gratefully acknowledge the technical and financial support provided by the Ministry of Education and King Abdulaziz University, Jeddah, Saudi Arabia. They also thank King Abdulaziz University Hospital and King Abdullah Medical City for approving and facilitating the sample collection.

### Authors' Contribution

Conceptualization, H.A., and S.D.; methodology, H.A., S.D., M.H., R.A., A.E., R.A.S., and M.H.; validation, H.A., Y.M.D., H.A.L., and E.B.Y.; formal analysis, H.A., M.Q., A.B., and F.A.; investigation, A.B., and F.A.; resources, H.A., and S.D.; writing original draft preparation, H.A., S.D., M.H., R.A., A.E., A.E., M.A., R.A.S., and E.B.Y.; writing review and editing, H.A., H.A.L., and E.B.Y.; visualization, H.A., and M.Q.; supervision, H.A., S.D., A.B., and F.A.; funding acquisition, A.R. All authors have read and agreed to the published version of the manuscript.

### Funding

This research work was funded by Institutional Fund Projects (grant No. IFPRC-034-140-2020).

### Ethics Approval

Patient samples were collected following the ethical approval by KAMC IRB registered at the National BioMedical Ethics Committee, King Abdulaziz City for Science and Technology (Registration No. H-02-K-001). Results from CEGMR molecular lab were used in compliance with Ethics approval obtained (Bio-ethical approval code: 01-CEGMR-Bioeth-2019).

### Informed Consent

An informed consent was obtained from all subjects involved in the study. As per international standards or university standards, the patient's written consent has been collected and preserved by the authors.

### Data Availability

The datasets generated and analyzed during the current study are available from the corresponding author upon reasonable request.

### ORCID ID

Heba Alkhatabi: 0000-0003-2097-2010  
Aisha Elaimi: 0000-0003-3214-4714  
Mohannad S Hazzazi: 0000-0002-6321-8248  
Majed N. Almashjary: 0000-0002-6619-0287  
Hind Alkhatabi: 0000-0002-8082-838X  
Yara Daoos: 0000-0003-1538-6770  
Elrashid B. Yasin: 0000-0002-4087-8112  
Ahmed Barefah: 0000-0003-2009-3817

### References

- 1) Nowell PC, Hungerford DA. Chromosome studies on normal and leukemic human leukocytes. *J Natl Cancer Inst* 1960; 25: 85-109.
- 2) Le Beau MM, Larson RA, Bitter MA, Vardiman JW, Golomb HM, Rowley JD. Association of an in-version of chromosome 16 with abnormal marrow eosinophils in acute myelomonocytic leukemia: a unique cytogenetic-clinicopathological association. *N Engl J Med* 1983; 309: 630-636.
- 3) Bollmann PW, Giglio AD. Chronic myeloid leukemia: past, present, future. *Einstein (Sao Paulo)* 2011; 9: 236-243.
- 4) Goldman JM. Chronic myeloid leukemia: a historical perspective. *Semin Hematol* 2010; 47: 302-311.
- 5) Koretzky GA. The legacy of the Philadelphia chromosome. *J Clin Invest* 2007; 117: 2030-2032.
- 6) Polampalli, S, Choughule, A, Negi, N, Shinde, S, Baisane, C, Amre, P, Subramanian, PG, Gujral, S, Prabhash, K, Parikh, P. Analysis and comparison of clinicohematological parameters and molecular and cyto-genetic response of two Bcr/Abl fusion transcripts. *Genet Mol Res* 2008; 7: 1138-1149.
- 7) Hochhaus, Andreas, Larson, Richard A, Guilhot, François, Radich, Jerald P, Branford, Su-

- san, Hughes, Timothy P, Bacarani, Michele, Deininger, Michael W, Cervantes, Francisco, Fujihara, Satoko. Long-term outcomes of imatinib treatment for chronic myeloid leukemia. *N Engl J Med* 2017; 376: 917-927.
- 8) Huang X, Kurata N, Wei X, Wang ZX, Wang A, Zhao Q, Zhao Y, Liu K, Lu H, Li W, Guo Y, Lu Y, Zhou C, Fan D, Weng Q, Zhu C, Huang T, Zhang L, Wang Y, Feng L, Furuumi H, Kubo T, Miyabayashi T, Yuan X, Xu Q, Dong G, Zhan Q, Li C, Fujiyama A, Toyoda A, Lu T, Feng Q, Qian Q, Li J, Han B. A map of rice genome variation reveals the origin of cultivated rice. *Nature* 2012; 490: 497-501.
- 9) Druker BJ, Talpaz M, Resta DJ, Peng B, Buchdunger E, Ford JM, Lydon NB, Kantarjian H, Capdeville R, Ohno-Jones S, Sawyers CL. Efficacy and safety of a specific inhibitor of the BCR-ABL tyrosine kinase in chronic myeloid leukemia. *N Engl J Med* 2001; 344: 1031-1037.
- 10) Jabbour E, Kantarjian H. Chronic myeloid leukemia: 2020 update on diagnosis, therapy and monitoring. *Am J Hematol* 2020; 95: 691-709.
- 11) Cortes J, Pavlovsky C, Saúbele S. Chronic myeloid leukaemia. *Lancet* 2021; 398: 1914-1926.
- 12) Jabbour EJ, Mendiola MF, Lingohr-Smith M, Lin J, Makenbaeva D. Economic modeling to evaluate the impact of chronic myeloid leukemia therapy management on the oncology care model in the US. *J Med Econ* 2019; 22: 1113-1118.
- 13) Eiring, Anna M, Page, Brent DG, Kraft, Ira L, Mason, Clinton C, Vellore, Nadeem A, Reseta, Diana, Zabriskie, Matthew S, Zhang, Tian Y, Khorashad, Jamshid S and Engar, Alexander J. Combined STAT3 and BCR-ABL1 inhibition induces synthetic lethality in therapy-resistant chronic myeloid leukemia. *Leukemia* 2015; 29: 586-597.
- 14) El-Missiry MA, Othman AI, El-Sawy MR, Lebede MF. Neuroprotective effect of epigallocatechin-3-gallate (EGCG) on radiation-induced damage and apoptosis in the rat hippocampus. *Int J Radiat Biol* 2018; 94: 798-808.
- 15) Shin MH, Kim J, Lim SA, Kim J, Kim SJ, Lee KM. NK cell-based immunotherapies in cancer. *Immune Netw* 2020; 20: e14.
- 16) Bacarani M, Rosti G, Soverini S. Chronic myeloid leukemia: the concepts of resistance and persistence and the relationship with the BCR-ABL1 transcript type. *Leukemia* 2019; 33: 2358-2364.
- 17) de Lavallade, Hugues, Finetti, Pascal, Carbuccia, Nadine, Khorashad, Jamshid S, Charbonnier, Aude, Foroni, Letizia, Apperley, Jane F, Vey, Norbert, Bertucci, François, Birnbaum, Daniel. A gene expression signature of primary resistance to imatinib in chronic myeloid leukemia. *Leuk Res* 2010; 34: 254-257.
- 18) Villuendas, R, Steegmann, JL, Pollan, M, Tracey, L, Granda, A, Fernandez-Ruiz, E, Casado, LF, Martínez, J, Martínez, P, Lombardía, L. Identification of genes involved in imatinib resistance in CML: a gene-expression profiling approach. *Leukemia* 2006; 20: 1047-1054.
- 19) Mughal TI, Psaila B, DeAngelo DJ, Saglio G, Van Etten RA, Radich JP. Interrogating the molecular genetics of chronic myeloproliferative malignancies for personalized management in 2021. *Hematologica* 2021; 106: 1787-1793.
- 20) Ercaliskan A, Eskazan AE. The impact of BCR-ABL transcript type on tyrosine kinase inhibitor responses and outcomes in patients with chronic myeloid leukemia. *Cancer* 2018; 124: 3806-3818.
- 21) Alves R, Gonçalves AC, Rutella S, Almeida AM, De Las Rivas J, Trougakos IP, Sarmento Ribeiro AB. Resistance to tyrosine kinase inhibitors in chronic myeloid leukemia—from molecular mechanisms to clinical relevance. *Cancers (Basel)* 2021; 13: 4820.
- 22) Amatu A, Sartore-Bianchi A, Siena S. NTRK gene fusions as novel targets of cancer therapy across multiple tumour types. *ESMO Open* 2016; 1: e000023.
- 23) Cocco E, Scaltriti M, Drilon A. NTRK fusion-positive cancers and TRK inhibitor therapy. *Nat Rev Clin Oncol* 2018; 15: 731-747.
- 24) Laetsch TW, Hong DS. Tropomyosin receptor kinase inhibitors for the treatment of TRK fusion cancer. *Clin Cancer Res* 2021; 27: 4974-4982.
- 25) Marchetti A, Felicioni L, Pelosi G, Del Grammasco M, Fumagalli C, Sciarrotta M, Malatesta S, Chella A, Barassi F, Mucilli F, Camplere P, D'Antuono T, Sacco R, Buttitta F. Frequent mutations in the neurotrophic tyrosine receptor kinase gene family in large cell neuroendocrine carcinoma of the lung. *Hum Mutat* 2008; 29: 609-616.
- 26) Iniguez-Ariza NM, Bible KC, Morris JC, Chintakuntlawar AV, Shridhar V, Smallridge RC, Meneff ME, Hilger C, Severson EA, Ryder MM. NTRK1-3 point mutations in poor prognosis thyroid cancers. *JCO* 2017; 35: 6087-6087.
- 27) Tomasson MH, Xiang Z, Walgren R, Zhao Y, Katsai Y, Miner T, Ries RE, Lubman O, Fremont DH, McLellan MD, Payton JE, Westervelt P, DiPersio JF, Link DC, Walter MJ, Graubert TA, Watson M, Baty J, Heath S, Shannon WD, Nagarajan R, Bloomfield CD, Mardis ER, Wilson RK, Ley TJ. Somatic mutations and germline sequence variants in the expressed tyrosine kinase genes of patients with de novo acute myeloid leukemia. *Blood* 2008; 111: 4797-4808.
- 28) Taylor J, Pavlick D, Yoshimi A, Marcelus C, Chung SS, Hechtman JF, Benayed R, Cocco E, Durham BH, Bitner L, Inoue D, Chung YR, Mulaney K, Watts JM, Diamond EL, Albacker LA, Mughal TI, Ebata K, Tuch BB, Ku N, Scaltriti M, Roshal M, Arcila M, Ali S, Hyman DM, Park JH, Abdel-Wahab O. Oncogenic TRK fusions are amenable to inhibition in hematologic malignancies. *J Clin Invest* 2018; 128: 3819-3825.
- 29) Hechtman JF, Benayed R, Hyman DM, Drilon A, Zehir A, Frosina D, Arcila ME, Dogan S, Klimstra DS, Ladanyi M, Jungbluth AA. Pan-Trk immunohistochemistry is an efficient and reliable screen

- for the detection of NTRK fusions. *Am J Surg Pathol* 2017; 41: 1547-1551.
- 30) Gatalica Z, Xiu J, Swensen J, Vranic S. Molecular characterization of cancers with NTRK gene fusions. *Mod Pathol* 2019; 32: 147-153.
- 31) Bertrand T, Kothe M, Liu J, Dupuy A, Rak A, Berne PF, Davis S, Gladysheva T, Valtre C, Crenne JY. The crystal structures of TrkA and TrkB suggest key regions for achieving selective inhibition. *J Mol Biol* 2012; 423: 439-453.
- 32) Sartore-Bianchi A, Ardini E, Bosotti R, Amatu A, Valtorta E, Somaschini A, Radrizzani L, Palmeri L, Banfi P, Bonazzina E, Misale S, Marrapese G, Leone A, Alzani R, Luo D, Hornby Z, Lim J, Veronese S, Vanzulli A, Bardelli A, Martignoni M, Davite C, Galvani A, Isacchi A, Siena S. Sensitivity to entrectinib associated with a novel LMNA-NTRK1 gene fusion in metastatic colorectal cancer. *J Natl Cancer Inst* 2015; 108: djv306.
- 33) Hsiao SJ, Zehir A, Sireci AN, Aisner DL. Detection of tumor NTRK gene fusions to identify patients who may benefit from tyrosine kinase (TRK) inhibitor therapy. *J Mol Diagn* 2019; 21: 553-571.
- 34) Zhou H, Xu R. Leukemia stem cells: the root of chronic myeloid leukemia. *Protein Cell* 2015; 6: 403-412.
- 35) Ly C, Arechiga AF, Melo JV, Walsh CM, Ong ST. Bcr-Abl kinase modulates the translation regulators ribosomal protein S6 and 4E-BP1 in chronic myelogenous leukemia cells via the mammalian target of rapamycin. *Cancer Res* 2003; 63: 5716-5722.
- 36) Sillaber C, Mayerhofer M, Böhm A, Vales A, Gruze A, Aichberger KJ, Esterbauer H, Pfeilstöcker M, Sperr WR, Pickl WF. Evaluation of antileukaemic effects of rapamycin in patients with imatinib, C, Mayer chronic myeloid leukaemia. *Eur J Clin Invest* 2008; 38: 43-52.
- 37) Steelman LS, Abrams SL, Whelan J, Bertrand FE, Ludwig DE, Bäscke J, Libra M, Stivala F, Milella M, Tafuri A, Lunghi P, Bonati A, Martelli AM, McCubrey JA. Contributions of the Raf/MEK/ERK, PI3K/PTEN/Akt/mTOR and Jak/STAT pathways to leukemia. *Leukemia* 2008; 22: 686-707.
- 38) Airiau K, Mahon F, Josselin M, Jeanneteau M, Belloc F. PI3K/mTOR pathway inhibitors sensitize chronic myeloid leukemia stem cells to nilotinib and restore the response of progenitors to nilotinib in the presence of stem cell factor. *Cell Death Differ* 2013; 4: e827-e.
- 39) Skorski T. Genomic instability: The cause and effect of BCR/ABL tyrosine kinase. *CHMR* 2007; 2: 69-74.
- 40) Spencer JA, Ferraro F, Roussakis E, Klein A, Wu J, Runnels JM, Zaher W, Mortensen LJ, Alt C, Turcotte R, Yusuf R, Côté D, Vinogradov SA, Scadden DT, Lin CP. Direct measurement of local oxygen concentration in the bone marrow of live animals. *Nature* 2014; 508: 269-273.
- 41) Zhang H, Li H, Xi HS, Li S. HIF1 $\alpha$  is required for survival maintenance of chronic myeloid leukemia stem cells. *Blood* 2012; 119: 2595-2607.
- 42) Machová Poláková K, Lopotová T, Klamová H, Burda P, Trněný M, Stopka T, Moravcová J. Expression patterns of microRNAs associated with CML phases and their disease related targets. *Mol Cancer* 2011; 10: 41.
- 43) Kotagama K, Chang Y, Mangone M. miRNAs as biomarkers in chronic myelogenous leukemia. *Drug Dev Res* 2015; 76: 278-285.